QUARTERLY JOURNAL
OF THE
ROYAL METEOROLOGICAL SOCIETY

Vol. 93 JANUARY 1967 No. 395

551.509.313 : 551.509.324.2 : 551.515.8

A 10-level atmospheric model and frontal rain

By F. H. BUSHBY and MARGARET S. TIMPSON
Meteorological Office, Bracknell

(Manuscript received 16 August 1966; in revised form 19 October 1966)

SUMMARY

A 10-level primitive equation model suitable for studying the dynamics of fronts and frontal rainfall is described. The atmosphere is assumed to be hydrostatic and inviscid and the effects of friction and topography are ignored. Latent heat due to evaporation and condensation is incorporated in the thermodynamic equation. No distinction is made between the ice and water stage and the atmosphere is assumed to be dry above 300 mb. The horizontal grid length is 40 km. The results of one 24-hr integration are described in detail.

1. INTRODUCTION

Numerical weather prediction has now reached the stage where forecasts of pressure patterns on the scale of anticyclones and depressions can be computed for up to three days ahead. Many National Meteorological Offices produce numerical forecasts which range in period from 24 to 72 hours and which vary from simple barotropic forecasts to those based on multi-level baroclinic models. Although some problems remain to be solved, the standard of these forecasts is as good as, if not better than, those produced by conventional methods. It is clear that numerical weather prediction can be advanced in two main ways; by extending the useful period of the forecast and by increasing the amount of detail in the forecast. This paper describes a numerical experiment designed to investigate atmospheric disturbances on the scale of fronts. This model has been developed for two main purposes; the study of the dynamics of fronts and the prediction of frontal rainfall.

Observations from the free atmosphere are available only from aerological sounding stations. These are separated by distances of at least several hundred kilometres and by very much greater distances over the oceans. Thus it is not possible to specify the detailed structure of fronts in the data which are used as the initial conditions for a forecast. It has been necessary to start the integrations from smooth but realistic fields of motion, temperature and humidity in the expectation that the characteristic concentration of gradients will develop gradually at the frontal surface if the problem has been properly formulated.

It is recognized that the quasi-geostrophic formulations of the dynamical equations become increasingly inaccurate as they are applied to systems with a scale less than 1,000 km. Ageostrophic motions are clearly very important in the vicinity of fronts and it is desirable to use the basic first order hydrodynamic and thermodynamic equations applicable to an inviscid hydrostatic atmosphere. These equations are frequently referred to in the literature as the primitive equations of motion. Charney (1955), Hinkelmann (1957, 1959) and Smagorinsky (1958, 1963) are among the early workers who demonstrated that it is possible to use the primitive equations in dynamical meteorology on the synoptic scale, whereas it had previously been thought that it was necessary to use the quasi-geostrophic approach in order to filter out unwanted noise from the equations.

The emphasis of the work reported in this paper is on the development of a model which is sufficiently realistic to give a reasonable estimate of frontal rainfall. The model should also be simple enough to enable the computation of 24 hr forecasts to be completed on computers which are likely to be available in the near future in time to be of use to a practising forecaster. Previous work on the computation of rainfall by the use of primitive equations, e.g. Manabe, Smagorinsky and Strickler (1965), and Smagorinsky and Staff Members (1965), has used finite difference schemes with a much longer grid length than that used in this work, and therefore has not been able to represent realistically the motion near fronts.

2. The model

(a) *General*

The atmosphere is represented by the model at 10 levels in the vertical at 100 mb intervals from 100 mb to 1,000 mb. Pressure is used as a vertical coordinate, and the horizontal coordinates are taken on a stereographic map projection. The state of the atmosphere at a given time is specified in the model by the height h of the pressure surfaces, the two components of wind u and v at each level and the humidity mixing ratio r of each of the seven 100 mb layers below 300 mb. The atmosphere is assumed to be dry above 300 mb and no distinction is made between the ice and water stage below 300 mb. The atmosphere is assumed to be hydrostatic and inviscid and the effects of friction and topography are ignored.

Humidity mixing ratio was chosen as the most suitable parameter for the representation of moisture. Smagorinsky and Collins (1955), Miyakoda (1956) and Manabe *et al.* (1965) also worked with this parameter, though their treatment of the precipitation process was quite different from that used in this model. In contrast, specific humidity was used for the representation of moisture by Komabayasi, Miyakoda, Aihara, Manabe and Katow (1955) and Aubert (1957).

The thermodynamic equation is expressed in terms of the thickness h' of 100 mb layers. In order to deal with condensation and evaporation effects it is necessary to know whether or not the air is saturated. The saturated humidity mixing ratio, r_s, of any 100 mb column is computed by evaluating a quartic polynomial of the thickness of the column. The coefficients of the polynomials, different for each layer, have been computed by fitting values of r_s and h' obtained from a tephigram to a quartic curve by the method of least squares. Quartic polynomials were found to give a very good representation of the actual relationship between r_s and h' which is much more complicated arithmetically, and this good representation extends over a much wider range of thickness than would be observed in the atmosphere.

If a column in a layer is not saturated then the humidity mixing ratio is changed by horizontal and vertical advection and by the evaporation of any water which is falling into that column from the column above. If the air is saturated and the rate at which moisture is arriving, both by advection and as liquid water from above, is greater than that required to keep the air saturated, allowing for changes in the temperature of the column, then any excess moisture is passed as liquid water into the column in the next layer below. The latent heat due to evaporation and condensation is included in the thermodynamic equation. Should, due to truncation or round-off errors, r become negative at a time t, then r is made zero. The humidity mixing ratio is also made equal to zero if the thickness of the layer is computed to be so low as to be outside the range for which the empirical formulae relating r_s to h' were derived.

(b) *The basic equations*

The motion is assumed to be frictionless and inviscid and the horizontal equations of motion are used in the form

$$\frac{\partial u}{\partial t} + m\left(u\frac{\partial u}{\partial x} + v\frac{\partial u}{\partial y} + g\frac{\partial h}{\partial x}\right) + \omega\frac{\partial u}{\partial p} - fv = 0, \quad . \quad . \quad (1)$$

$$\frac{\partial v}{\partial t} + m\left(u\frac{\partial v}{\partial x} + v\frac{\partial v}{\partial y} + g\frac{\partial h}{\partial y}\right) + \omega\frac{\partial v}{\partial p} + fu = 0, \quad . \quad . \quad (2)$$

where m is the map magnification factor $\sec^2(\pi/4 - \theta/2)$, θ being the latitude, $\omega \equiv dp/dt$ and f is the Coriolis parameter.

The equation of continuity is used in the form

$$\frac{\partial \omega}{\partial p} + m\left(\frac{\partial u}{\partial x} + \frac{\partial v}{\partial y}\right) = 0. \quad . \quad . \quad . \quad . \quad . \quad (3)$$

It is recognized that Eq. (3) ignores the effect of the convergence of the meridians, but this effect is small in short period forecasts.

If M_A is defined as the rate of transfer of liquid water into a layer from the layer above and M_B is defined as the rate of transfer of liquid water from a layer into the layer below, then M, the rate of condensation in the layer, is defined by

$$M = M_B - M_A, \quad . \quad . \quad . \quad . \quad . \quad . \quad (4)$$

and M will be negative for evaporation. The atmosphere is assumed dry above 300 mb and $M_A \equiv 0$ for the layer from 300 to 400 mb.

If $r < r_s$, $\partial r/\partial t$ is given by

$$\left(\frac{\partial r}{\partial t}\right)_{\text{DRY}} = -m\left(u\frac{\partial r}{\partial x} + v\frac{\partial r}{\partial y}\right) + M_A - \omega\frac{\partial r}{\partial p}, \quad . \quad . \quad (5)$$

and $$M_B = 0. \quad . \quad . \quad . \quad . \quad . \quad . \quad . \quad (6)$$

If $r \geqslant r_s$

$$\frac{\partial r}{\partial t} = \frac{\partial r_s}{\partial t} = \frac{\partial h'}{\partial t}\frac{dr_s}{dh'}, \quad . \quad . \quad . \quad . \quad . \quad (7)$$

and $$M_B = \left(\frac{\partial r}{\partial t}\right)_{\text{DRY}} - \frac{\partial r_s}{\partial t}, \quad . \quad . \quad . \quad . \quad . \quad (8)$$

unless M_B thus computed is negative, when

$$\frac{\partial r}{\partial t} = \left(\frac{\partial r}{\partial t}\right)_{\text{DRY}}, \quad . \quad . \quad . \quad . \quad . \quad . \quad (9)$$

and $$M_B = 0. \quad . \quad . \quad . \quad . \quad . \quad . \quad . \quad (10)$$

The thermodynamic equation can be written as

$$\frac{\partial h'}{\partial t} + m\left(u\frac{\partial h'}{\partial x} + v\frac{\partial h'}{\partial y}\right) + \omega\frac{\partial h'}{\partial p} + \frac{\omega h'}{\gamma p} - \frac{100\,(\gamma - 1)\,ML}{g\,\gamma\,p} = 0, \quad . \quad (11)$$

where L is the coefficient of latent heat of condensation and γ is the ratio of the specific heats. If $r \geqslant r_s$ then, substituting from Eq. (4), Eqs. (8) and (11) are solved simultaneously for M_B and $\partial h'/\partial t$. If M_B is negative then Eqs. (9) and (10) apply and Eq. (11) has to be solved for $\partial h'/\partial t$.

The tendency equation, using the hydrostatic approximation and taking the vertical velocity $w \equiv dz/dt = 0$ at mean sea-level, since topography is ignored, can be written as

$$\frac{\partial h_{10}}{\partial t} = \frac{\omega_G}{g\rho} - m\left(u_G\frac{\partial h_{10}}{\partial x} + v_G\frac{\partial h_{10}}{\partial y}\right), \quad . \quad . \quad . \quad (12)$$

where the subscript G refers to values at *MSL* and the subscript 10 refers to values at 1,000 mb. Values of u_G and v_G were obtained by linear extrapolation from corresponding values at 900 and 1,000 mb, and values of ω_G were obtained by extrapolating values of $\partial\omega/\partial p$

linearly from 900 and 1,000 mb to *MSL* and subsequent integration. Eq. (11) gives the rate of change of thickness of each layer of the model and can be used in conjunction with Eq. (12) to give the rate of change of the height of each of the pressure surfaces.

(c) *Finite difference approximations and boundary conditions*

A finite difference scheme is used which is similar to that described by Eliassen (1956). The essential feature of this scheme is that it is staggered both in time and space. Dependent variables are kept only at alternate horizontal grid points; u is kept at grid points midway between adjacent values of h in the y direction, v is kept between adjacent values of h in the x direction, and ω is evaluated at the central points of a 2 grid length square, which has a value of h at each of the corners. Values of a dependent variable at odd time steps are computed at grid points diagonally adjacent to the points at which the variable is known at an even time step. The horizontal grid consists of 95×63 points approximately 40 km apart and there are 10 levels in the vertical.

There appears to be little virtue in introducing complicated difference schemes in order to conserve momentum, energy or mass when the integrations are only made for a 24 hr period. Simple three point centred differences are used for the space derivatives, apart from the vertical derivatives in Eqs. (1), (2) and (11) at the top and bottom of the model. Here, one-sided differences are used except in Eq. (11) at the top of the model. A one-sided difference is a bad approximation to $\partial h'/\partial p$ at 150 mb since the thickness of 100 mb layers is increasing rapidly in this region, the thickness of the 100 mb layer above 100 mb being infinite. It was therefore decided to use a value for $\partial h'/\partial p$ at 150 mb based on the ICAN atmosphere, correcting for the temperature of the layer by taking

$$\left(\frac{\partial h'}{\partial p}\right)_{150} = \left(\frac{\partial h'}{\partial p}\right)_{150,\ \text{ICAN}} \frac{h'_{150}}{h'_{150,\ \text{ICAN}}} \quad . \quad . \quad . \quad . \quad (13)$$

When in the non-linear terms a variable or its derivative is required at a grid point at which it is not available, a simple average is taken of the values at neighbouring grid points at which the quantity required has been computed. Phillips (1962) showed that Eliassen's scheme introduces sufficient smoothing to ensure computational stability. Phillips also indicated that if a simple centred difference formula is used for the time derivatives, then the nature of the equations is such that two distinct computational modes are set up, one for odd and one for even time steps, and computational instability can arise from this. The following system of integrating with respect to time has been adopted for all variables

$$H_{t+\delta t} = H_t + \left(\frac{\partial H}{\partial t}\right)_t \delta t, \quad . \quad . \quad . \quad . \quad (14)$$

$$H_{t+2\,\delta t} = H_t + 2\left(\frac{\partial H}{\partial t}\right)_{t+\delta t} \delta t, \quad . \quad . \quad . \quad (15)$$

where the suffix t relates to any even time step. This process when used in conjunction with Eliassen's scheme is computationally stable for the linearized equations providing δt is sufficiently small, but it must be emphasized that this system of integrating with respect to time is unstable unless some form of spatial smoothing similar to that implicit in Eliassen's scheme is introduced. In order to satisfy the stability criterion for fast moving gravity waves it is necessary to use a time step of 108 sec, 800 time-steps being necessary for a 24 hr forecast.

The vertical velocity at each level is obtained by integrating Eq. (3) with respect to p by using the trapezium rule. The boundary condition at 100 mb is taken as

$$\omega_{100} = 50\left(\frac{\partial \omega}{\partial p}\right)_{100}, \quad . \quad . \quad . \quad . \quad . \quad (16)$$

which is consistent with $\omega = \partial\omega/\partial p = 0$ at $p = 0$, a realistic boundary condition.

One of the biggest difficulties in this project has been the control of spuriously large accelerations and divergences near the lateral boundaries. Most of the other workers in this field have taken the lateral boundaries as streamlines. This is clearly realistic if one is working on the scale of the hemisphere (Smagorinsky, Manabe and Holloway 1965), or if one is dealing with an equatorial belt (Shuman and Vanderman 1966), but it is most unrealistic if one is dealing with a relatively small section of the Northern Hemisphere. It should be emphasized that one is not so much trying to represent actual events at the boundary, but rather to prevent rapid amplification of spurious fast-moving waves near the boundary which would quickly ruin the calculations for the complete area.

It is sufficient to specify the normal component of velocity, the height of the pressure surfaces, and the humidity mixing ratio on the boundary for all even time steps.

The first calculations were performed, for the sake of simplicity, with these quantities kept constant with respect to time. These calculations became unstable after about 6 hours forecast time with the rapid amplification of spurious divergences near the boundary, although elsewhere the divergence patterns were relatively smooth. This fault was cured by first computing the new wind field inside the boundary, computing the divergence field where possible using the new wind field and extrapolating linearly this divergence field to the points one grid length inside the boundary. The normal component of wind on the boundary can then be computed from Eq. (3).

At even time steps the component of acceleration normal to the boundary is computed from Eqs. (1) and (2) at points one grid length inside the boundary. The growth of spurious accelerations at points of inflow across the boundary can be prevented by ensuring that these values are no larger than they were at the previous even time step. This can be done by decreasing the pressure gradient term in Eqs. (1) and (2) by reducing the height of the pressure surface on the boundary by an appropriate amount.

(*d*) *Initial data*

The initial data consist of geopotential heights and humidity mixing ratios at the standard pressure levels, although no moisture parameter is included at levels above 400 mb. Simple interpolation formulae are used where necessary to obtain geopotential heights at

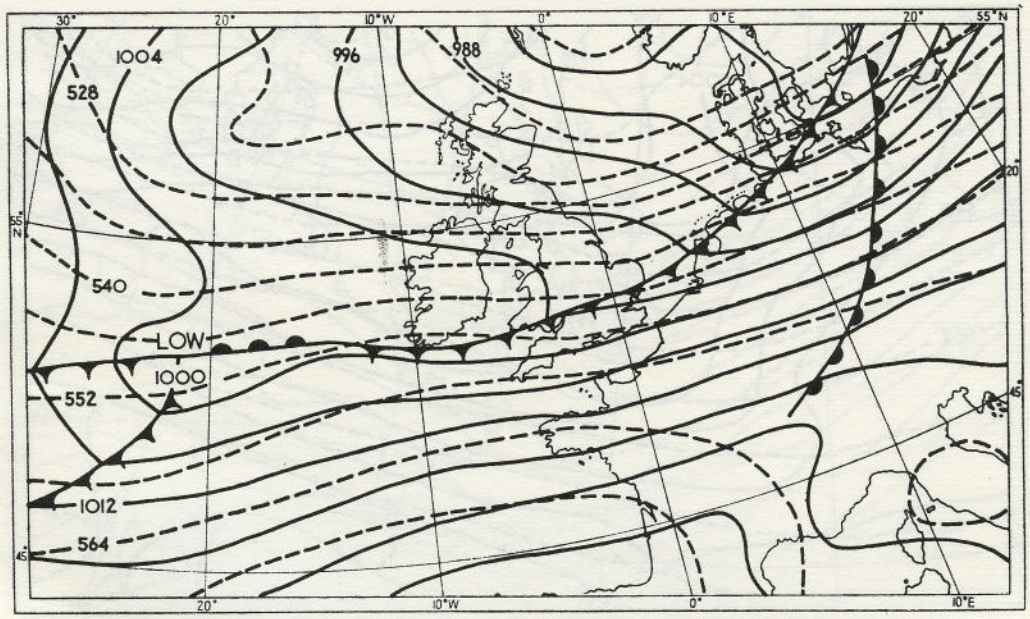

Figure 1. Actual Synoptic Situation 0000 GMT 1 December 1961.
surface isobars ———— 500 mb contours - - - - - -

100 mb intervals from 1,000 mb to 100 mb and humidity mixing ratios at 100 mb intervals from 950 mb to 350 mb, it being appropriate for the moisture parameter to be carried at the mid-point of each 100 mb layer. The initial wind fields are assumed to be non-divergent and are computed from the initial height fields by solving

$$\nabla^2 \psi = \frac{mg}{f} \nabla^2 h, \qquad (17)$$

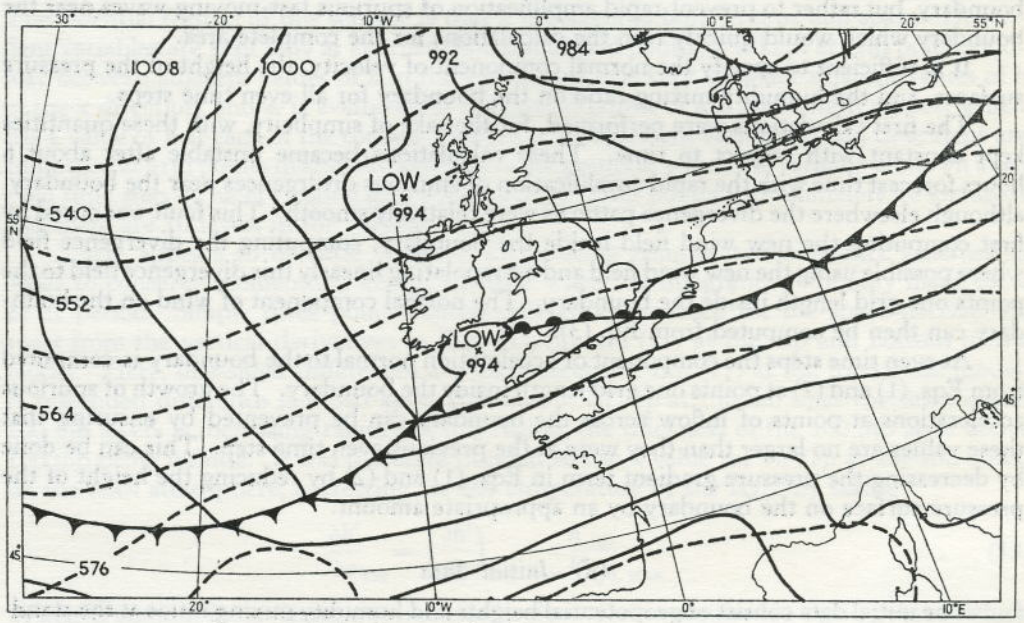

Figure 2. Actual Synoptic Situation 1200 GMT 1 December 1961.
surface isobars ——— 500 mb contours - - - - - - -

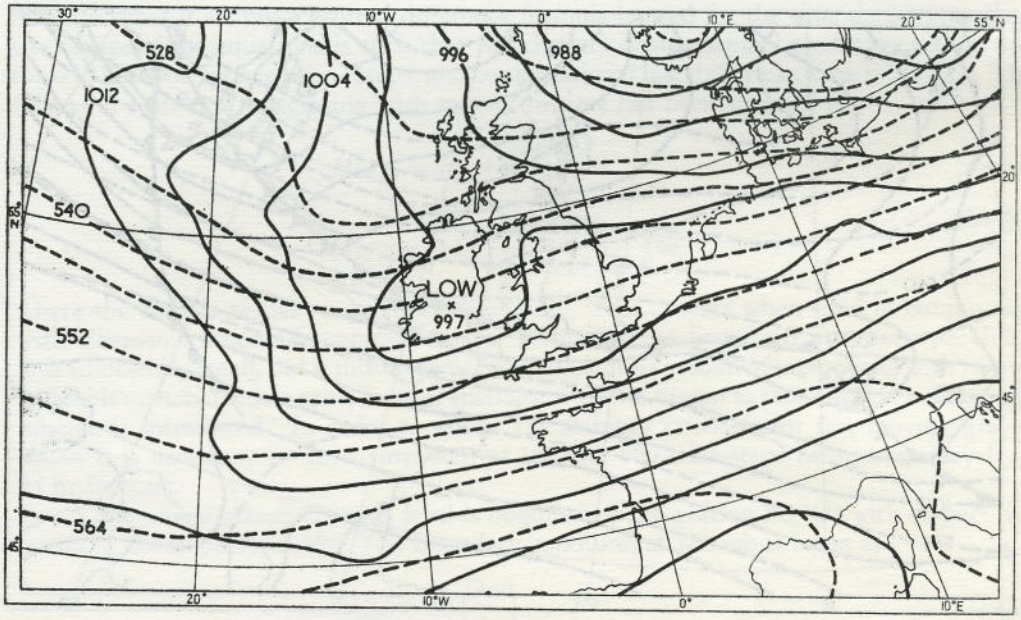

Figure 3. 12 hr Forecast of Synoptic Situation 1200 GMT 1 December 1961.
surface isobars ——— 500 mb contours - - - - - - -

$$u = -\frac{\partial \psi}{\partial y}, \quad . \quad . \quad . \quad . \quad . \quad . \quad (18)$$

$$v = \frac{\partial \psi}{\partial x}, \quad . \quad . \quad . \quad . \quad . \quad . \quad (19)$$

at each level. A suitable boundary condition for Eq. (17) is to assume the normal component

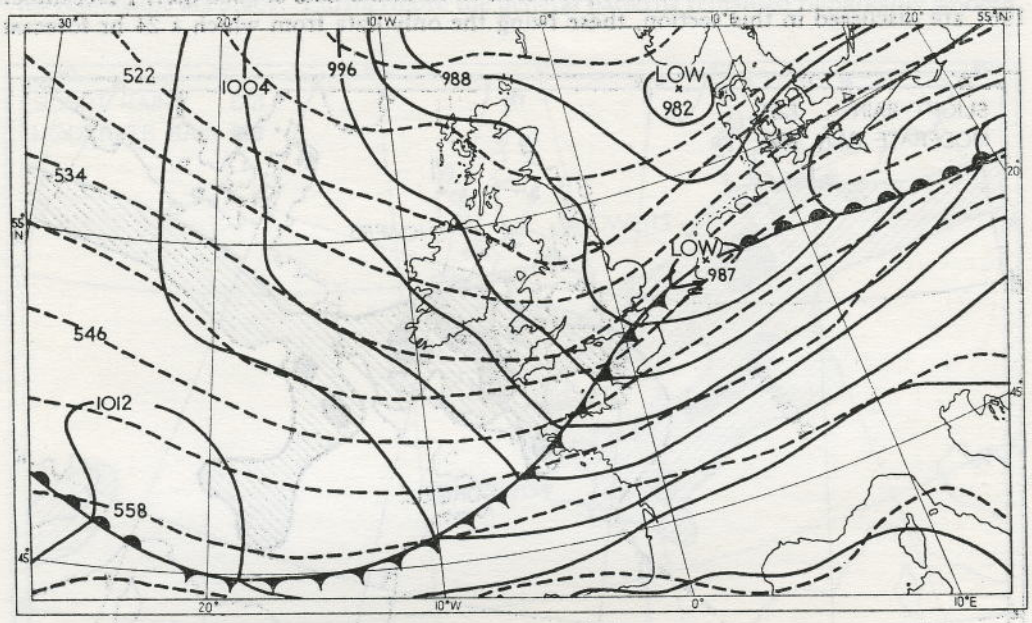

Figure 4. Actual Synoptic Situation 0000 GMT 2 December 1961.
surface isobars ——— 500 mb contours - - - - - -

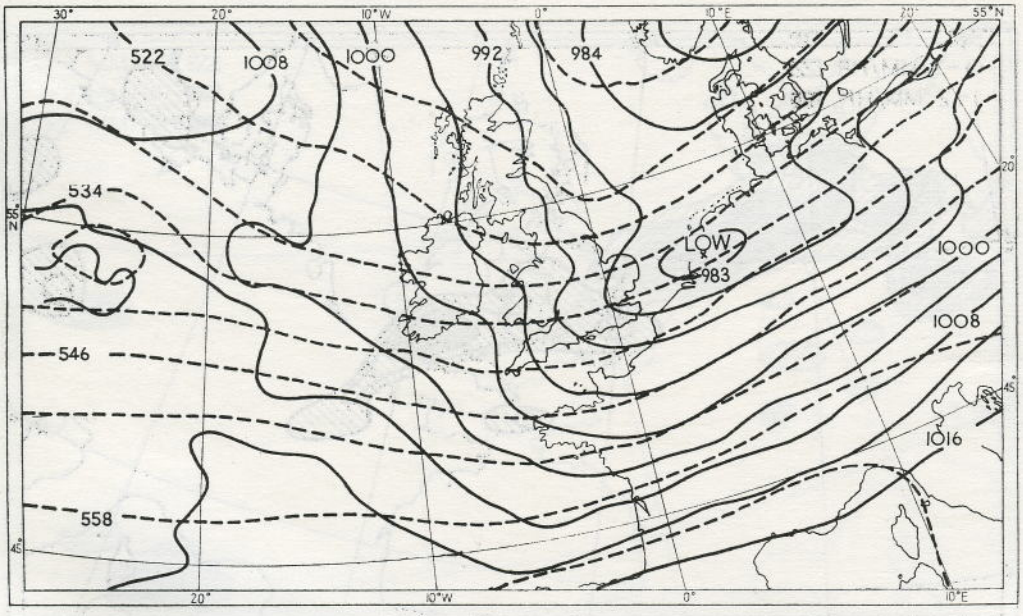

Figure 5. 24 hr Forecast of Synoptic Situation 0000 GMT 2 December 1961.
surface isobars ——— 500 mb contours - - - - - -

of velocity to be as nearly geostrophic as possible. This derivation of winds from contour heights has in effect removed the divergence effect of the Coriolis parameter and map projection from the geostrophic wind and ensures that the point divergences computed by simple centred finite differences are zero initially.

3. Results

The results of the 24 hr forecast produced from initial data at 0000 GMT, 1 December 1961 are discussed in this section, these being the only data from which a 24 hr forecast

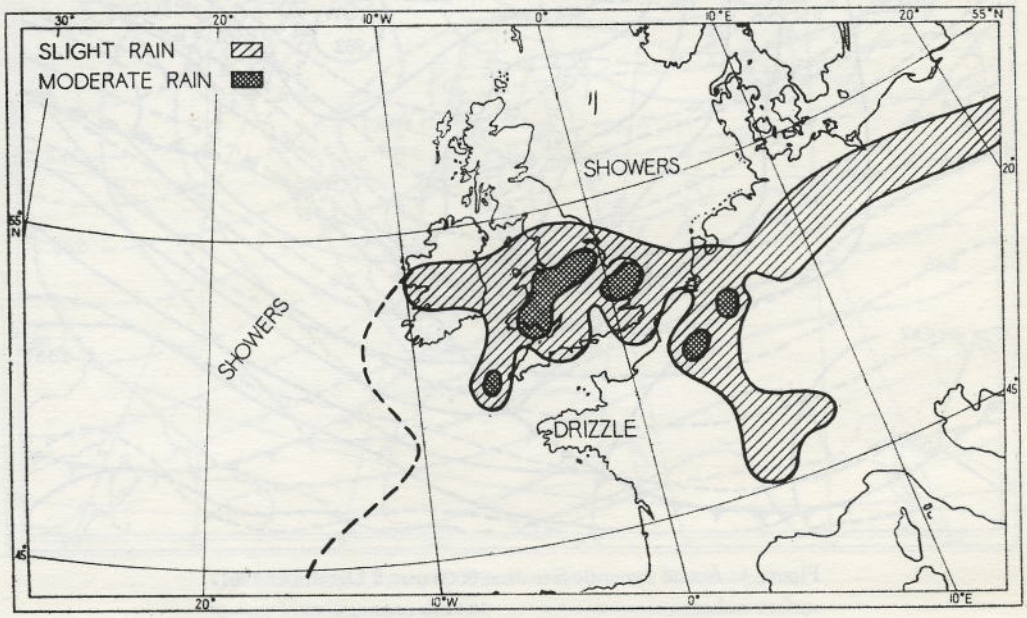

Figure 6. Present Weather 1200 GMT 1 December 1961.

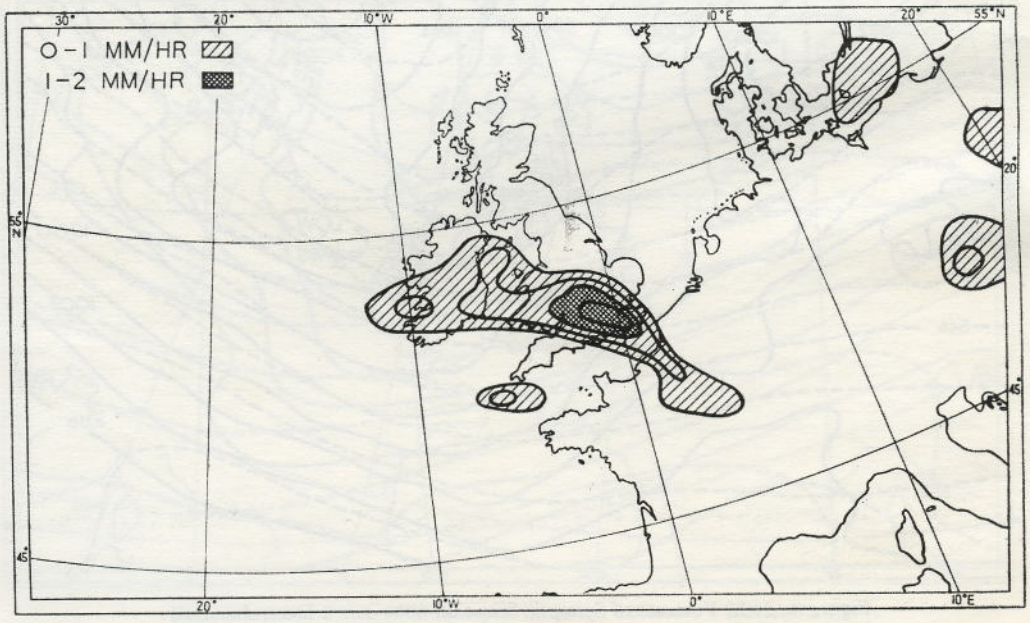

Figure 7. Forecast Rate of Rainfall mm/hour 1200 GMT 1 December 1961.

has so far been completed. In the results illustrated in Figs. 1 to 11, the outer 12 boundary rows of grid points have been excluded. From a synoptic viewpoint the results are, on the whole, very good. There is good agreement between the forecast and actual surface and 500 mb patterns after 12 hours (Figs. 2 and 3), and this is maintained in the 24 hr forecast (Figs. 4 and 5).

In particular the position of the centre of the small wave depression which moved across southern Britain and the associated cold and warm front surface troughs were forecast with reasonable accuracy. Furthermore the general patterns remained remarkably smooth,

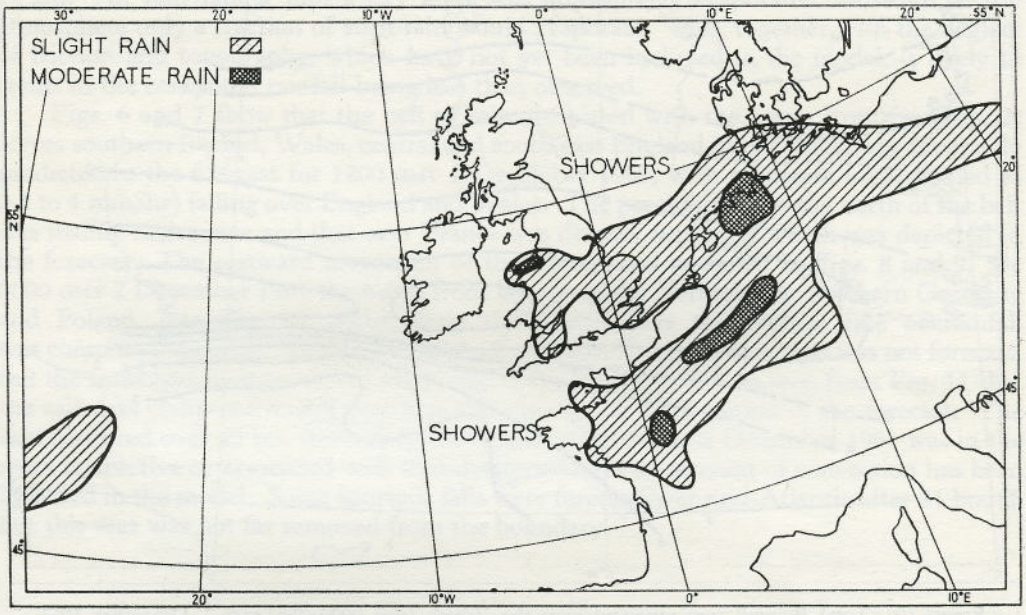

Figure 8. Present Weather 0000 GMT 2 December 1961.

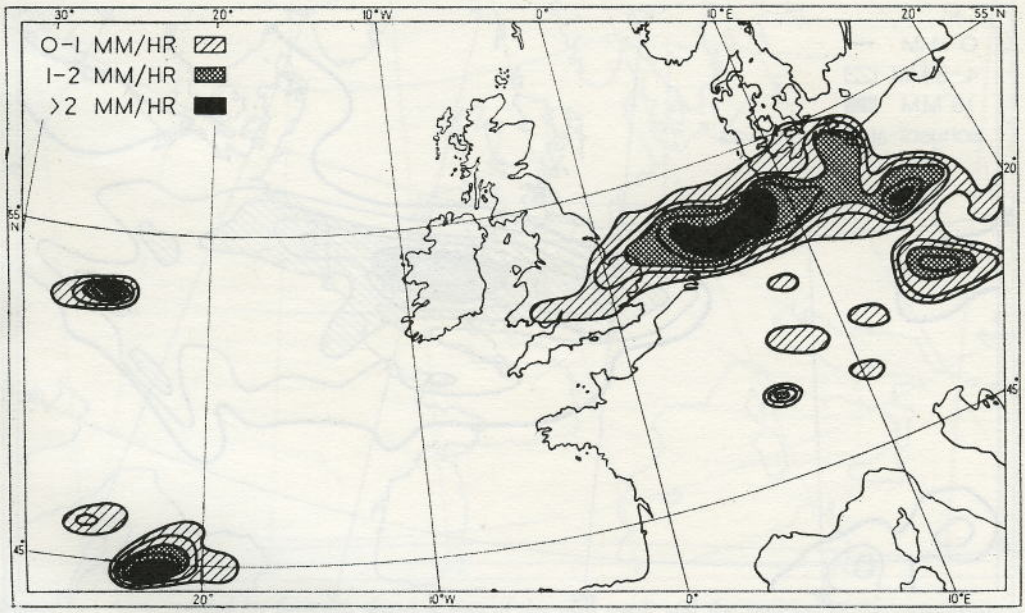

Figure 9. Forecast Rate of Rainfall mm/hour 0000 GMT 2 December 1961.

although no smoothing other than that implicit in the finite difference scheme has been introduced into the computation. The deepening of the wave depression was accurately forecast but the results show some discrepancies in the values of the pressure centres, the computed value of the centre of the wave depression being 3 mb too high after 12 hours and about 3 mb too low after 24 hours. These discrepancies are partly due to a small amplitude oscillation of about 2 mb with a period of 4 to 5 hours and a wavelength much

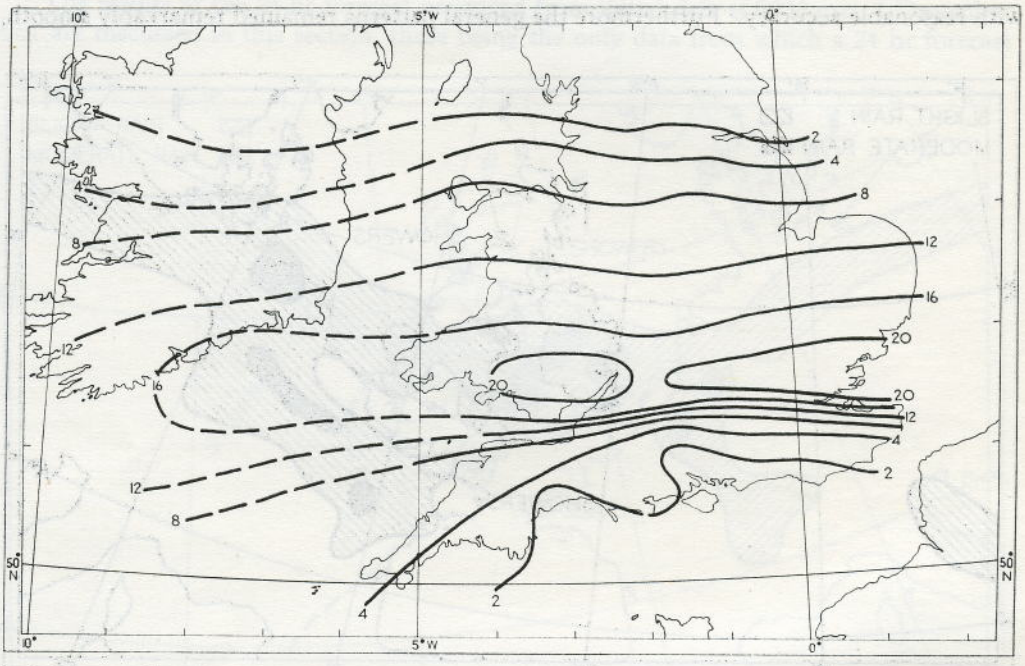

Figure 10. Total Rainfall mm observed over the British Isles 0000-2400 GMT 1 December 1961 (Irish totals 0600-1800 GMT).

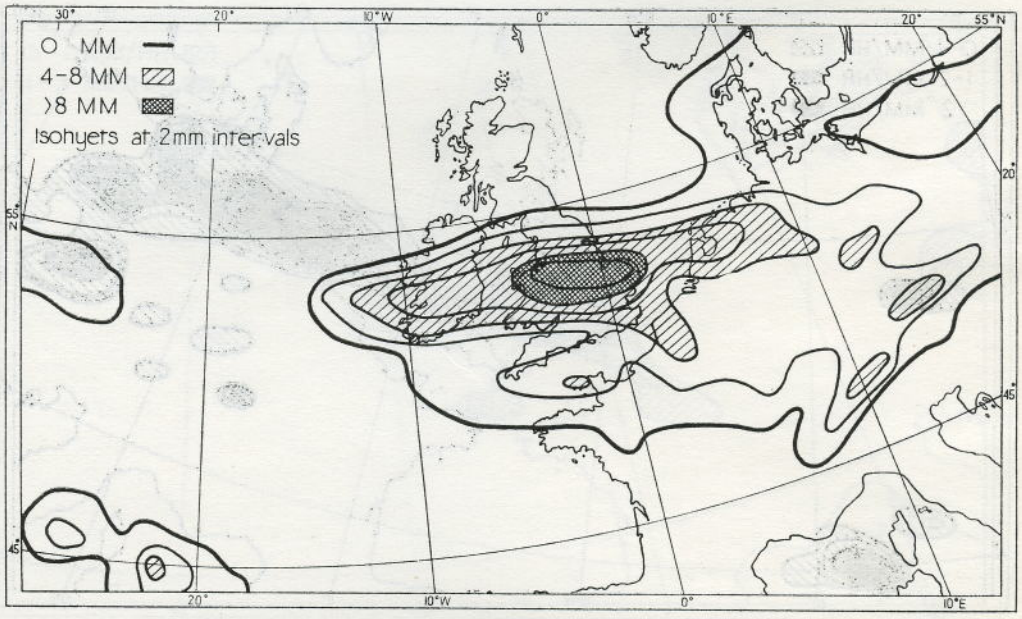

Figure 11. Forecast Total Rainfall mm 0000-2400 GMT 1 December 1961.

greater than the synoptic scale. Similar oscillations have been detected in 3 other 12 hour forecasts and the effect is possibly due to a gravity wave. However, there has been no evidence of an increase in the amplitude of this spurious wave and its presence does not appear to affect the synoptic value of the forecasts.

The computed rates of rainfall for 12 and 24 hours ahead are illustrated in Figs. 7 and 9 respectively, and the total rainfall computed for the 24 hours in Fig. 11. The forecast patterns were derived from grid points spaced 40 km apart and therefore could not include the smaller scale patterns and locally large totals of rain, which are evident in the actual rainfall charts over those areas where the network of rainfall observations was closer than 40 km. All rain falling into a dry layer was immediately evaporated, although in the atmosphere only a fraction of such rain would evaporate. This, together with the neglect of friction and topography, which have not yet been included in the model, is likely to result in the computed rainfall being less than observed.

Figs. 6 and 7 show that the belt of rain associated with the warm front (see Fig. 2) across southern Ireland, Wales, central and south east England into France, was accurately predicted in the forecast for 1200 GMT 1 December 1961, with moderate rain (defined as 0·5 to 4 mm/hr) falling over England and Wales. The precipitation to the north of the belt was mainly convective and that over France was drizzle, neither of which was depicted in the forecast. The eastward movement of the frontal rain is shown in Figs. 8 and 9. By 0000 GMT 2 December 1961 the warm front lay across the Netherlands, northern Germany and Poland, (see Fig. 4), which were the areas where the highest rate of rainfall was computed to occur. The slight rain over northern France at this time was not forecast, but the front had by then moved some distance away and it will be seen from Fig. 11 that the rain was computed to fall over this area during the 24 hr period of the forecast. The rain observed over all but south and east Britain at 0000 GMT 2 December 1961 was in the main convective or associated with thunderstorms, and no account of convection has been included in the model. Some spurious falls were forecast over mid-Atlantic after 24 hours, but this area was not far removed from the boundary.

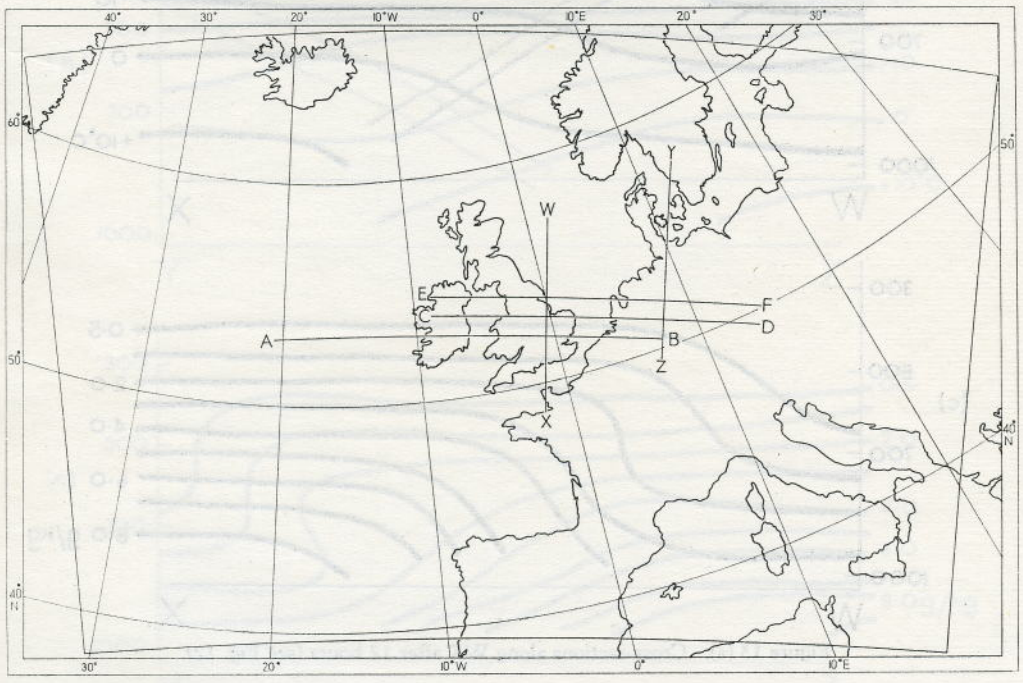

Figure 12. Area covered by forecast, showing size of the grid used, and the position of the cross-sections illustrated in Figs. 13 and 14.

Comparing the actual and forecast totals (Figs. 10 and 11) over the British Isles, the axis of the forecast area of heaviest rain was displaced somewhat northwards into the Midlands of England, but the position of the limit of rainfall over Northern Ireland and northern England was very adequately predicted.

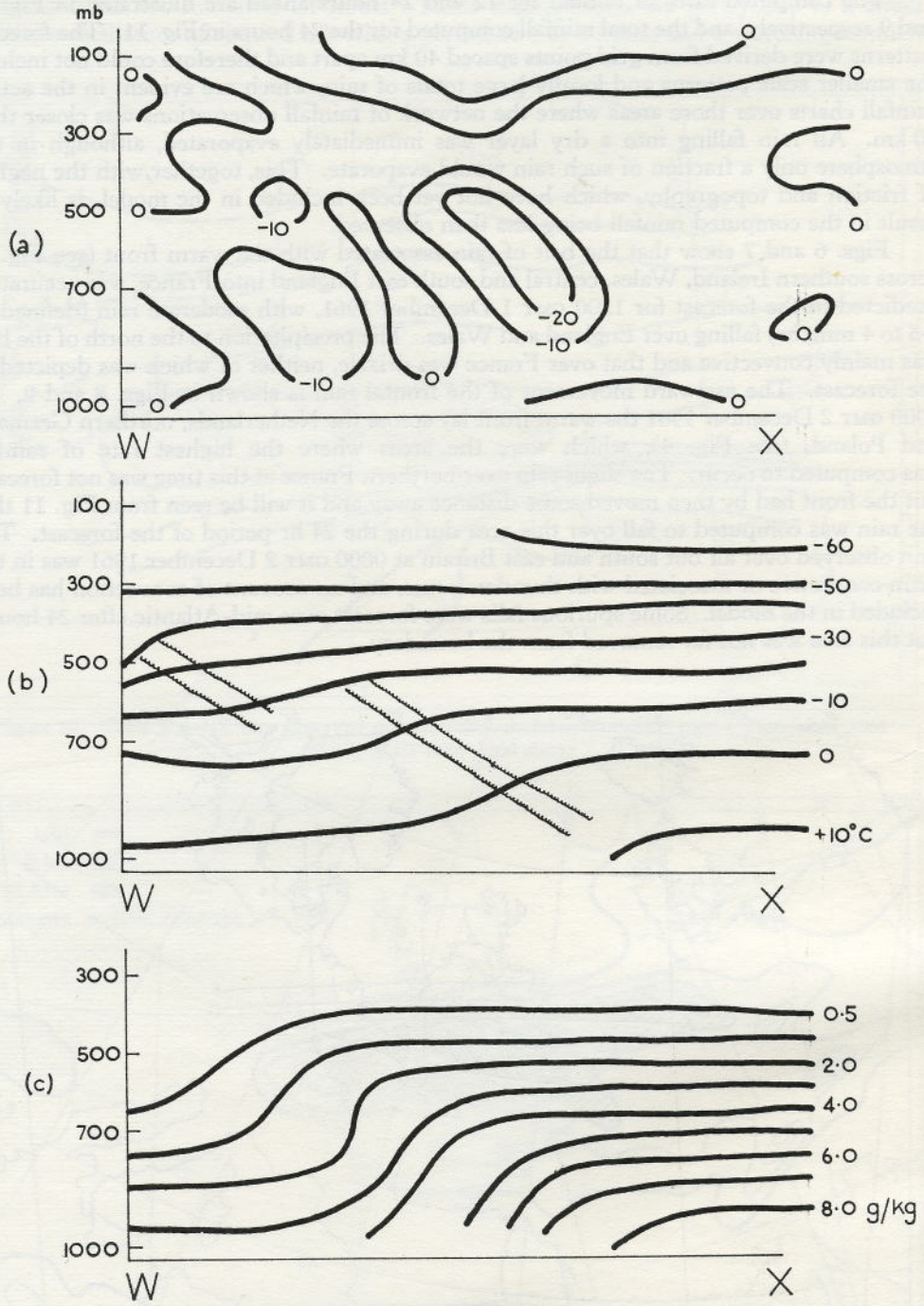

Figure 13 (a). Cross-sections along WX after 12 hours (see Fig. 12).

(a) Vertical motion (mb/hour)
(b) Isotherms (°C), wavy lines indicate zone of greatest horizontal temperature gradient
(c) Humidity Mixing Ratio (gm/kg)

The frontal characteristics can be studied most satisfactorily from vertical cross-sections along and normal to the front. Figs. 13 (a) and 13 (b) show vertical cross-sections well ahead of the small surface wave depression and normal to the warm front at 1200 GMT 1 December 1961 and at 0000 GMT 2 December 1961 respectively. The temperature cross-sections were derived from the mean temperatures for each 100 mb layer computed from the appropriate 100 mb thickness. As far as can be judged the patterns of vertical motion,

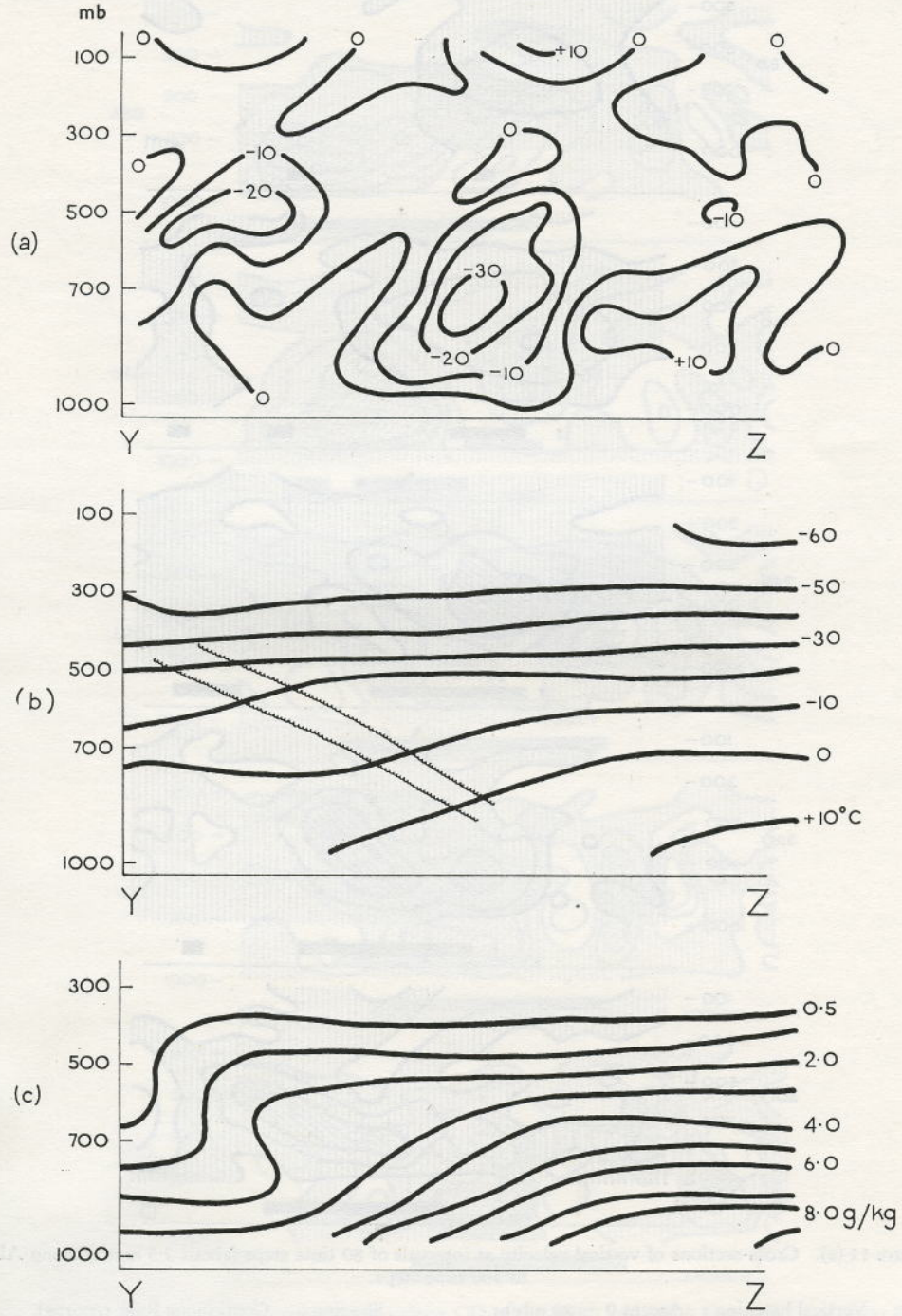

Figure 13 (b). As Fig. 13 (a) with cross-sections along YZ after 24 hours.

temperature and humidity mixing ratio are consistent with observed characteristics o warm fronts. From the mean temperature cross-sections the slope of the warm fron would appear to have been of the order of 1 in 50.

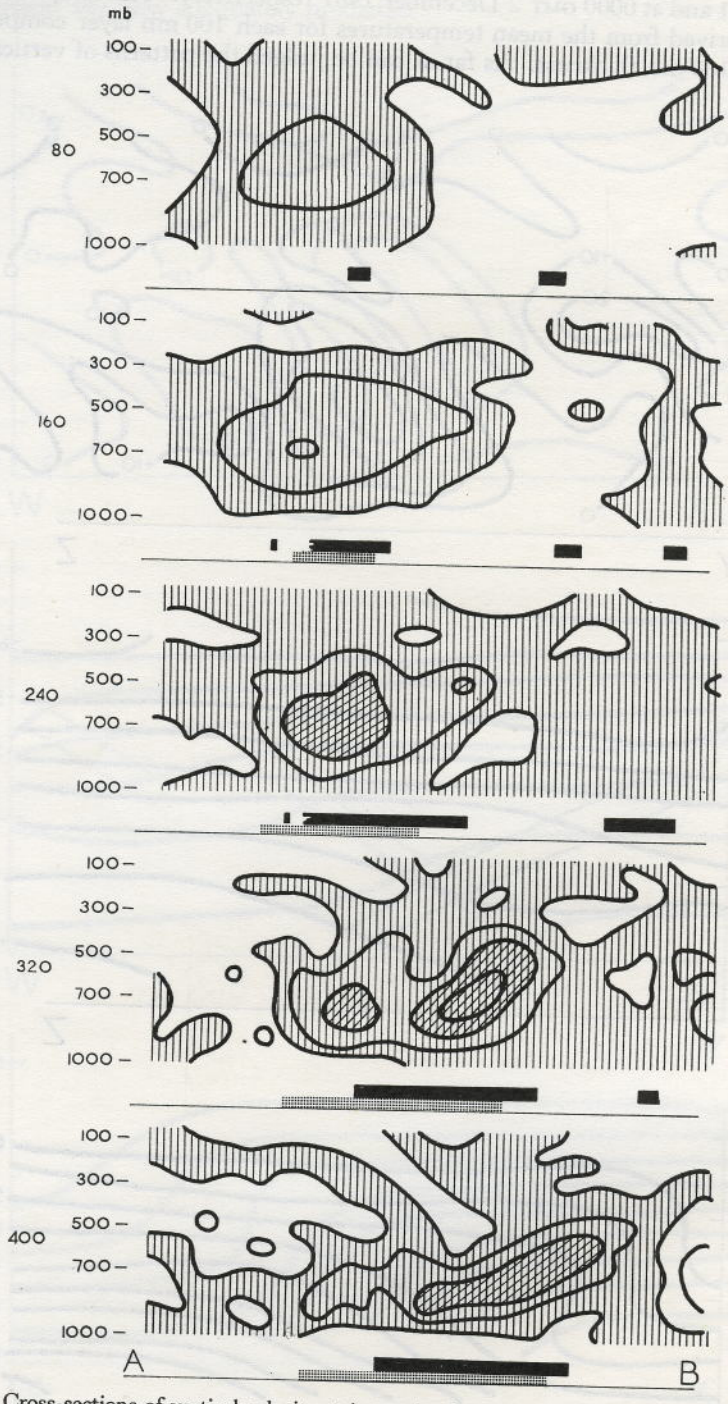

Figure 14 (a). Cross-sections of vertical velocity at intervals of 80 time steps (about 2·5 hours) along AB up to 400 time steps.

Vertical hatching : Ascent 0 — 20 mb/hr.
Cross hatching : Ascent > 20 mb/hr.
Shading : Continuous Rain reported.
Stippling : Computed rain.

A picture of the development of the vertical velocities along the front is illustrated by Figs. 14 (a) and (b). The predicted rainfall associated with upward vertical motion from about the 6 hr forecast was of a scale which was in close agreement with that of the continuous rain areas taken from the actual charts. The vertical velocities at 1,000 mb remain acceptably small throughout the computations, but it will be seen that roughness

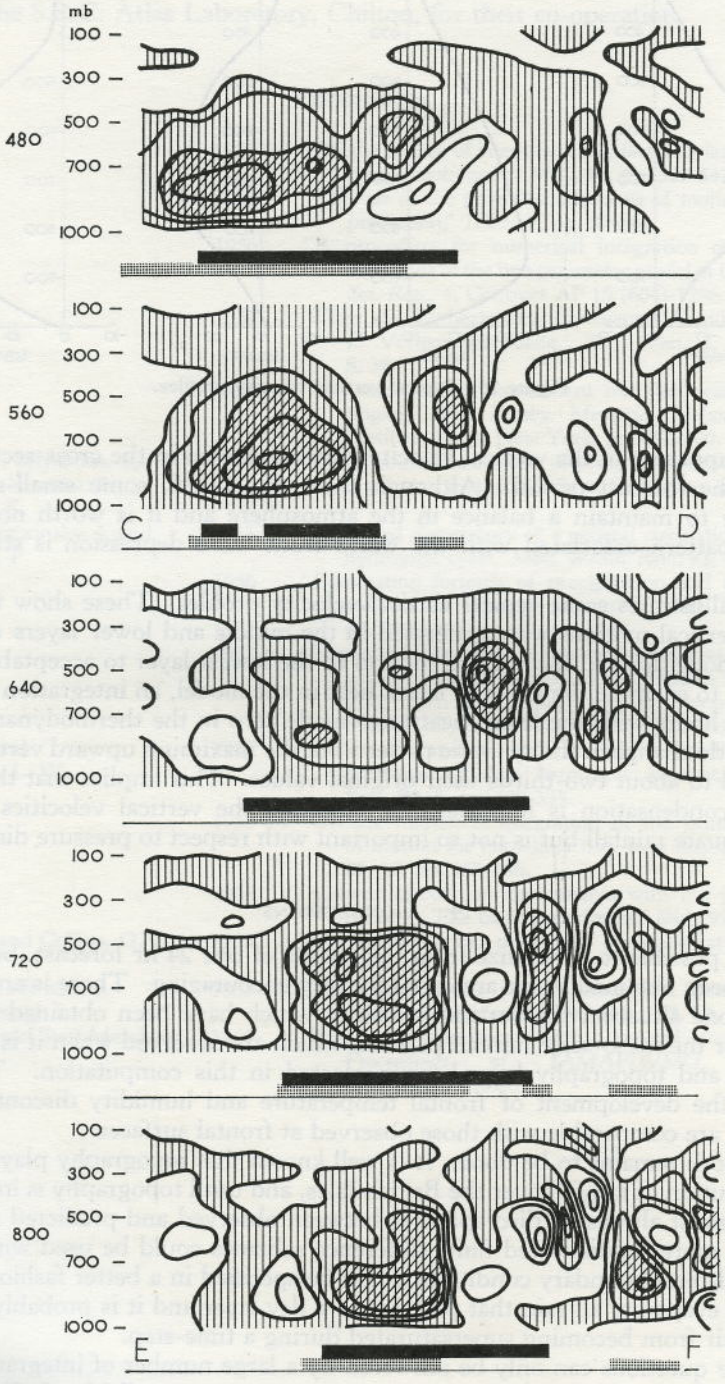

Figure 14 (b). As Fig. 14 (a) with cross-sections along CD at the 480th and 560th time steps and along EF at the 640th, 720th and 800th time steps.

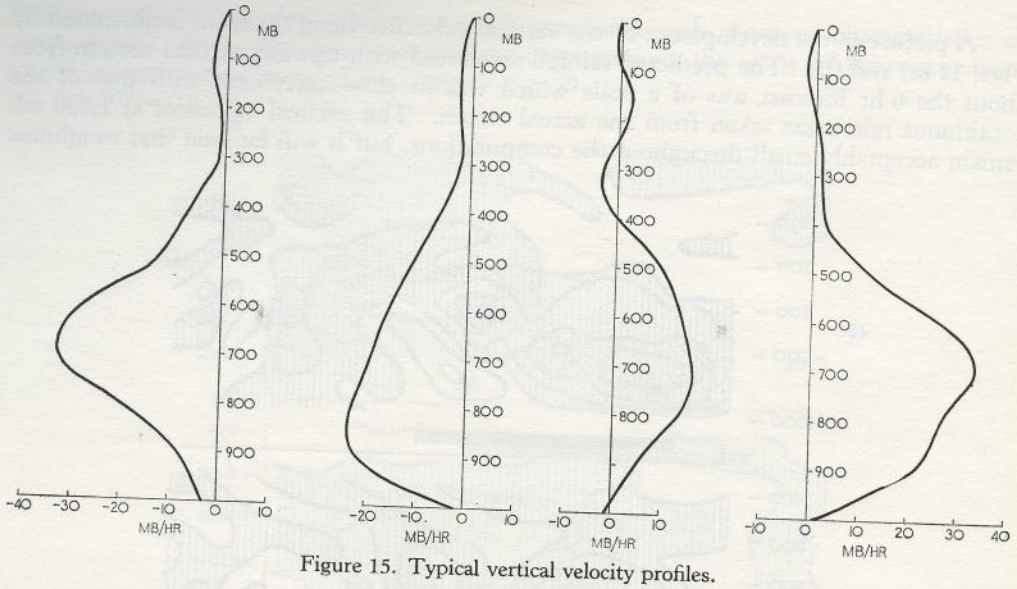

Figure 15. Typical vertical velocity profiles.

is becoming apparent in the vertical velocity patterns shown in the cross-sections towards the end of the forecast period. Although these are unreal, some small-scale features are necessary to maintain a balance in the atmosphere and it is worth noting that the larger-scale pattern associated with the warm front wave depression is still reasonably smooth.

Fig. 15 illustrates some typical vertical velocity profiles. These show that although quite large vertical motions were generated in the middle and lower layers of the troposphere, the model limited the vertical motion in the lowest layer to acceptable values.

In order to examine the effect of latent heat in the model, an integration was repeated from 6 to 12 hours with the latent heat term made zero in the thermodynamic equation. There was little change in the synoptic pattern but the maximum upward vertical velocities were reduced to about two-thirds their original values. This implies that the latent heat released by condensation is important in obtaining the vertical velocities sufficient to produce adequate rainfall but is not so important with respect to pressure distributions.

4. Conclusions

It is not possible to generalize from the results of one 24 hr forecast, but the results which have been obtained so far are certainly very encouraging. There is ample evidence that in this one situation the vertical velocities which have been obtained are sufficient to account for the meso-scale rainfall patterns which are observed when it is remembered that friction and topography have been neglected in this computation. There is also evidence of the development of frontal temperature and humidity discontinuities with slopes which are comparable with those observed at frontal surfaces.

Much work remains to be done. It is well known that topography plays a large part in the distribution of rainfall over the British Isles, and until topography is included in the model there must always be discrepancies between observed and predicted rainfall. It is possible that more sophisticated finite difference schemes could be used with advantage, and that the lateral boundary conditions could be specified in a better fashion. It may be better not to evaporate all rain that passes into a dry layer and it is probably desirable to prevent the air from becoming supersaturated during a time-step.

All these questions can only be answered by a large number of integrations, each of which takes several hours on the fastest computers at present available. Suffice to say that the results obtained so far justify the continuation of these numerical experiments.

Acknowledgments

We wish to acknowledge the permission of the Director-General of the Meteorological Office to publish this paper, and the assistance given by Mr. G. R. R. Benwell in interpreting the synoptic implication of the results. The authors also wish to thank the Director and staff of the S.R.C. Atlas Laboratory, Chilton, for their co-operation.

References

Aubert, E. J. 1957 'On the release of latent heat as a factor in large-scale atmospheric motions,' *J. Met.*, **14**, pp. 527-542.

Charney, J. 1955 'The use of the primitive equations of motion in numerical prediction,' *Tellus*, **7**, pp. 22-26.

Eliassen, A. 1956 'A procedure for numerical integration of the primitive equations of the two parameter model of the atmosphere,' *Sci. Rep.*, 4, Contract AF 19 (604)-1286.

Hinkelmann, K. 1957 'Uber die Einbeziehung divergenter Wind Komponenten in Vorhersagemodelle,' *Ber. Wetterd. Bad Kissingen*, **5**, 38.

1959 'Ein numerisches Experiment mit den primitiven Gleichungen,' *The Rossby Memorial Volume*, Rockefeller Institute Press, New York, pp. 486-500.

Komabayasi, M., Miyakoda, K., Aihara, M., Manabe, S. and Katow, K. 1955 'The quantitative forecast of precipitation with the numerical prediction method,' *J. Met. Soc. Japan*, **33**, 5, pp. 25-36.

Manabe, S., Smagorinsky, J. and Strickler, R. F. 1965 'Simulated climatology of a general circulation model with a hydrologic cycle,' *Mon. Weath. Rev.*, **93**, 12, pp. 769-798.

Miyakoda, K. 1956 'Forecasting formula of precipitation and the problem of conveyance of water vapour,' *J. Met. Soc., Japan*, **34**, pp. 212-225.

Phillips, N. A. 1962 'Numerical integration of the hydrostatic system of equations with a modified version of the Eliassen finite difference grid,' *Met. Soc. Japan*, Proc. Int. Symp. Num. Weath. Pred., Tokyo, Nov. 7-13 1960, pp. 109-119.

Shuman, F. G. and Vanderman, L. W. 1966 'Difference system and boundary conditions for the primitive equation barotropic forecast,' *Mon. Weath. Rev.*, **94**, 5, pp. 329-335.

Smagorinsky, J. 1958 'On the numerical integration of the primitive equations of motion for baroclinic flow in a closed region,' *Ibid.*, **86**, 12, pp. 457-466.

1963 'General circulation experiments with the primitive equations. 1. The basic experiment,' *Ibid.*, **91**, 3, pp. 99-165.

Smagorinsky, J. and Collins, G. O. 1955 'On the numerical prediction of precipitation,' *Ibid.*, **83**, pp. 53-68.

Smagorinsky, J., Manabe, S. and Holloway, J. L. 1965 'Numerical results from a nine-level general circulation model of the atmosphere,' *Ibid.*, **93**, 12, pp. 727-768.

Smagorinsky, J. and Staff Members 1965 'Prediction experiments with a general circulation model,' *Proceedings of IAMAP/WMO*, International Symposium, Moscow.